Catalytic performance and mechanism of a Pt/TiO$_2$ catalyst for the oxidation of formaldehyde at room temperature

Changbin Zhang [a], Hong He [a,*], Ken-ichi Tanaka [b]

[a] State Key Laboratory of Environmental Chemistry and Ecotoxicology, Research Center for Eco-Environmental Sciences, Chinese Academy of Sciences, Beijing 100085, China
[b] Saitama Institute of Technology, 1690 Fusaiji, Okabe, Saitama, Japan

Abstract

The performance of TiO$_2$ supported noble metal (Pt, Rh, Pd and Au) catalysts was examined and compared for the catalytic oxidation of formaldehyde (HCHO). Among them, the Pt/TiO$_2$ was the most active catalyst. The effects of Pt loading and gas hourly space velocity (GHSV) on Pt/TiO$_2$ activity for HCHO oxidation were investigated at a room temperature (20 °C). The optimal Pt loading is 1 wt.%. At this loading, HCHO can be completely oxidized to CO$_2$ and H$_2$O over the Pt/TiO$_2$ in a GHSV of 50,000 h^{-1} at 20 °C. The 1% Pt/TiO$_2$ was characterized using BET, XRD, high resolution (HR) TEM and temperature programmed reduction (TPR) methods. The XRD patterns and HR TEM image show that Pt particles on TiO$_2$ are well dispersed into a size smaller than 1 nm, an important feature for the high activity of the 1% Pt/TiO$_2$. The mechanism of HCHO oxidation was studied with respect to the behavior of adsorbed species on Pt/TiO$_2$ surface at room temperature using in situ DRIFTS. The results indicate that surface formate and CO species are the main reaction intermediates during the HCHO oxidation. The formate species could decompose into adsorbed CO species on the catalyst surface without the presence of O$_2$, and the CO was then oxidized to CO$_2$ with the presence of O$_2$. Based on these results, a simplified mechanism for the catalytic oxidation of HCHO over 1% Pt/TiO$_2$ was proposed.
© 2006 Elsevier B.V. All rights reserved.

Keywords: Formaldehyde; Noble metal; Pt/TiO$_2$; Formate species; In situ DRIFTS

1. Introduction

Formaldehyde (HCHO) emitted from building and furnishing materials and consumer products is one of dominating volatile organic compounds (VOCs) in the indoor environment [1]. HCHO is known to cause nasal tumors, irritation of the mucous membranes of the eyes and respiratory tract, and skin irritation [2]. Because of the increasing concern on HCHO in the indoor environment, the abatement of HCHO is of significant practical interest at low temperature, especially at room temperature.

A number of studies related to the removal of HCHO have been carried out using potassium permanganate, activated carbon, aluminum oxide, some ceramic materials and a board-like air-cleaning material consisting of activated carbon particles and manganese oxides as adsorbents both in the laboratory and in the field [3–5]. Generally, these absorbents successfully reduced indoor concentrations of HCHO at field experiments, but these absorbents were effective for only a short period due to their limited removal capacities.

Catalytic oxidation is one of the most promising technologies for the VOCs abatement because VOCs can be oxidized to CO$_2$ over catalysts at much lower temperatures than those of thermal oxidation [6–8]. The conventional catalysts of catalytic oxidation reaction include the supported noble metal (Pt, Pd, Rh and Au) catalysts [7–12] and metal oxides (Ag, Cu, Cr and Mn) [13–20]. Saleh and Hussian [13] investigated the surface decomposition of HCHO on clean and oxidized films of Ni, Pd and Al, and detected an emission of carbon dioxide gas, subsequent to the dissociative adsorption of HCHO on oxidized films above 150 °C. Imamura et al. [14] have found that silver–cerium composite oxide was active for oxidative decomposition of HCHO above 150 °C. Álvarez-Galván et al. [15] have reported that HCHO could be completely oxidized into CO$_2$ and H$_2$O over 0.4 wt.% Pd–Mn/Al$_2$O$_3$ above 90 °C. If catalytic oxidative decomposition of HCHO occurs over catalysts at

* Corresponding author. Tel.: +86 10 62849123; fax: +86 10 62923563.
E-mail address: honghe@rcees.ac.cn (H. He).

room temperature, the technology can be very useful for the removal of indoor HCHO without thermal and photon sources. In evaluation of the removal efficiencies of several metal oxides for HCHO in a static reaction vessel, Sekine [20] found that manganese oxide could react with HCHO and release carbon dioxide even at room temperature. However, the low efficiency of manganese oxide for HCHO oxidation to CO_2 at room temperature has limited its application for the removal of indoor HCHO. Therefore, the development of an oxidation catalyst for effective HCHO decomposition at room temperature is still a challenge.

Recently, we reported a high efficient Pt/TiO_2 catalyst over which HCHO can be completely oxidized into CO_2 and H_2O at room temperature [21]. This indicates that TiO_2 is a favorable support material for the low temperature oxidation of HCHO. In the present work, we studied the TiO_2 supported noble metal (Pt, Rh, Pd and Au) catalysts for the oxidation of HCHO, and found that the Pt/TiO_2 was the most active catalyst among them. Then we further characterized the Pt/TiO_2 using BET, XRD, high resolution TEM and TPR methods. In addition, we proposed the reaction mechanism of the catalytic oxidation of HCHO based on the results of in situ DRIFTS carried out over Pt/TiO_2 at room temperature.

2. Experimental

2.1. Catalyst preparation

The TiO_2 supported 1 wt.% noble metal (Pt, Rh, Pd and Au) catalysts were prepared by an impregnation method with an anatase type TiO_2 (Wako Pure Chemicals) and an aqueous solution of $AuCl_4$, $RhCl_3$, $Pd(NO_3)_2$ or H_2PtCl_6, respectively. After impregnation, the excessive water was removed in a rotary evaporator at 80 °C. The samples were dried at 110 °C for 12 h and then calcined at 400 °C for 2 h. Pretreatments of TiO_2 supported noble metal catalysts were applied to obtain a steady-going catalytic performance.

2.2. Characterization of catalyst

The nitrogen adsorption–desorption isotherms were obtained at −196 °C over the whole range of relative pressures, using a Micromeritics ASAP2000 automatic equipment on samples degassed at 220 °C. Specific areas were calculated from these isotherms by applying the BET method and taking a value of 0.162 nm^2 for the cross-section of the physically adsorbed nitrogen molecule. The fresh catalysts were characterized by X-ray diffractometry using a computerized Rigaku D/max-RB X-Ray Diffractometer (Japan, Cu Kα radiation, 1.54056 nm). High resolution TEM (HR TEM) images were obtained by employing a JEOL-3010 device with 300 kV accelerating voltage.

A Micromeritics TPR 2900 apparatus was used for the temperature programmed reduction (TPR) analysis. Reduction profiles were obtained by passing a flow with 5% H_2/Ar at a rate of 50 cm^3 min^{-1} (STP) through the sample (weight around 50 mg). The temperature was increased from 25 to 500 °C at a heating rate of 10 °C min^{-1}, and the amount of hydrogen consumed was determined on a thermal conductivity detector (TCD) as a function of temperature. The TCD signal was calibrated using CuO (Spex) as a standard.

2.3. In situ DRIFTS

In situ DRIFTS spectra were recorded in a NEXUS 670-FTIR equipped with a smart collector and a liquid N_2 cooled MCT detector. The sample (about 30 mg) for study was finely ground and placed in a ceramic crucible. A flow of feed gas mixture was controlled by mass flow meters. All spectra were measured with a resolution of 4 cm^{-1} and accumulating 100 scans. A background spectrum was subtracted from each spectrum.

2.4. Activity test of catalysts

The activity tests for the catalytic oxidation of HCHO over the catalysts were performed in a fixed-bed quartz flow reactor with a gas mixture containing 100 ppm HCHO, 20 vol% O_2 and He balanced at a total flow rate of 50 cm^3 min^{-1}. With the change of catalyst volume, the gas hourly space velocities (GHSV) were equivalent to 50,000, 100,000 and 200,000 h^{-1}. HCHO standard gas was constantly introduced from a gas-generator system [5]. The HCHO, CO and CO_2 were analyzed on-line using a gas chromatograph (GC) equipped with hydrogen flame ionization detector (FID) and Ni catalyst converter which was used for converting carbon oxides and HCHO quantitatively into methane in the presence of hydrogen before the detector. The separations of the reactants and products were achieved using two columns: a carbon molecular sieve column for permanent gases (CO and CO_2) and a GDX-403 column for the HCHO. The operating parameters were as
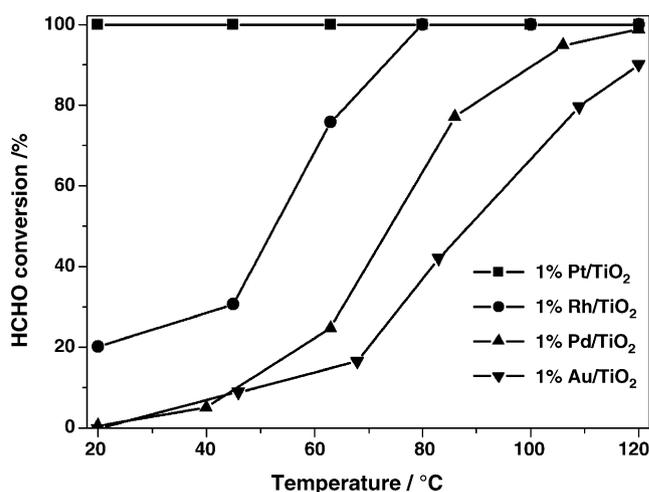
Fig. 1. HCHO conversions on TiO_2 supported 1 wt.% noble metal (Pt (■); Rh (●); Pd (▲); Au (▼)) catalysts at various temperatures. Reaction conditions: HCHO 100 ppm, O_2 20 vol%, He balance, total flow rate 50 cm^3 min^{-1}, GHSV 50,000 h^{-1}.
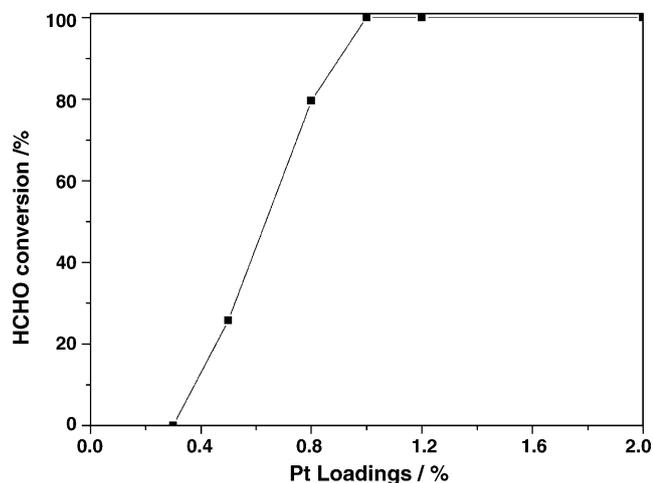
Fig. 2. HCHO conversions on Pt/TiO₂ catalysts with various Pt loadings at room temperature (20 °C). Reaction conditions: HCHO 100 ppm, O₂ 20 vol%, He balance, total flow rate 50 cm³ min⁻¹, GHSV 50,000 h⁻¹.
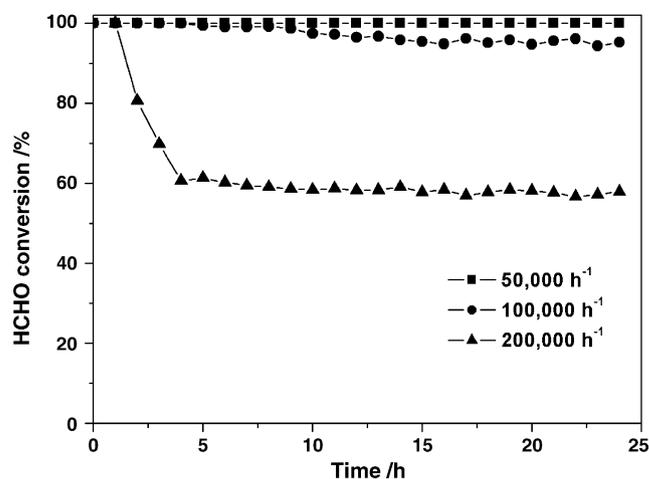
Fig. 3. HCHO conversions as a function of reaction time on 1% Pt/TiO₂ at room temperature at various GHSVs of 50,000 h⁻¹ (■), 100,000 h⁻¹ (●) and 200,000 h⁻¹ (▲). Reaction conditions: HCHO 100 ppm, O₂ 20 vol%, He balance, total flow rate 50 cm³ min⁻¹.

Table 1
Mass balance table of the activity test over 1% Pt/TiO₂ at room temperature

Gas	SV = 50,000 h⁻¹			SV = 100,000 h⁻¹			SV = 200,000 h⁻¹		
	Inlet (ppm)	Outlet (ppm)	Yield^a (%)	Inlet (ppm)	Outlet (ppm)	Yield^a (%)	Inlet (ppm)	Outlet (ppm)	Yield^a (%)
HCHO	102	0	–	101	3	–	102	43	–
CO₂	5.2	107.2	100	4.9	103.6	99.7	4.8	63.7	99.8
CO	3.2	3.2	–	2.9	2.9	–	2.4	2.4	–

^{a} Yield (%) = ΔCO_2 (ppm) × 100/$\Delta HCHO$ (ppm), $n = 10$.

follows: temperature of the detector, 180 °C; temperature of the column, 50 °C; carrier gas, helium 30 cm⁻³ min⁻¹; volume of the analyzed sample, 1 ml.

3. Results and discussion

3.1. Activity test

3.1.1. Effect of noble metals

The catalytic activities of the TiO₂ supported 1% noble metal (Pt, Rh, Pd or Au) catalysts were evaluated for HCHO oxidation and the results are shown in Fig. 1. It is evident that the activity of 1% noble metals/TiO₂ for HCHO oxidation follows the order of Pt/TiO₂ ≫ Rh/TiO₂ > Pd/TiO₂ > Au/TiO₂. The Pt/TiO₂ showed a very high activity, and HCHO could be completely oxidized over the Pt/TiO₂ catalyst in a GHSV of 50,000 h⁻¹ even at room temperature, while pure TiO₂ had no activity for HCHO oxidation to CO₂ at the same reaction conditions.

Table 2
Specific area of TiO₂ and 1% Pt/TiO₂ catalysts

Sample	BET area (m²/g)
TiO₂	49.7
1% Pt/TiO₂	47.4

3.1.2. Effect of Pt loading

Based on the results above, we focused study on the TiO₂ supported Pt catalyst for HCHO oxidation. The effect of Pt loading on the activity of Pt/TiO₂ for HCHO oxidation was studied at room temperature (20 °C) and the result is shown in Fig. 2. The 0.3% Pt/TiO₂ showed no activity for HCHO oxidation. Increasing the Pt loading from 0.3 to 1% enhanced the HCHO conversion over the Pt/TiO₂ up to 100% at room
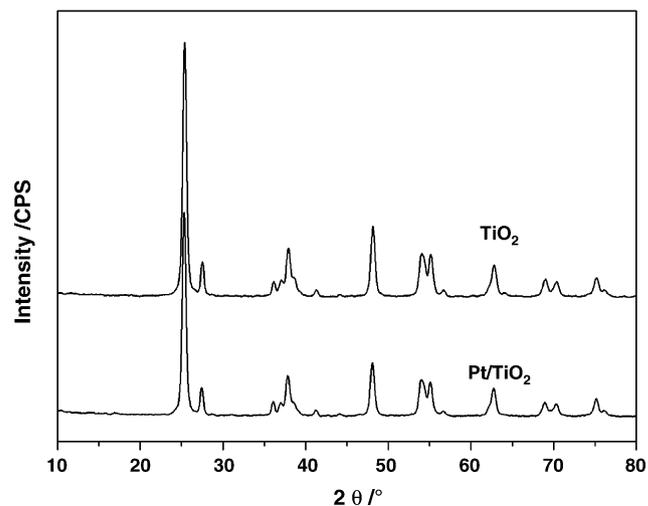
Fig. 4. X-ray diffraction patterns of TiO₂ and 1% Pt/TiO₂ catalysts.
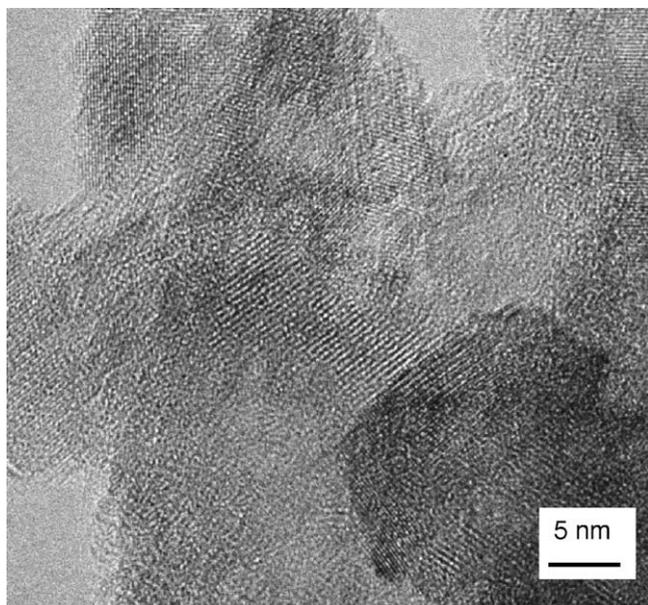
Fig. 5. High resolution TEM image of 1% Pt/TiO$_2$.
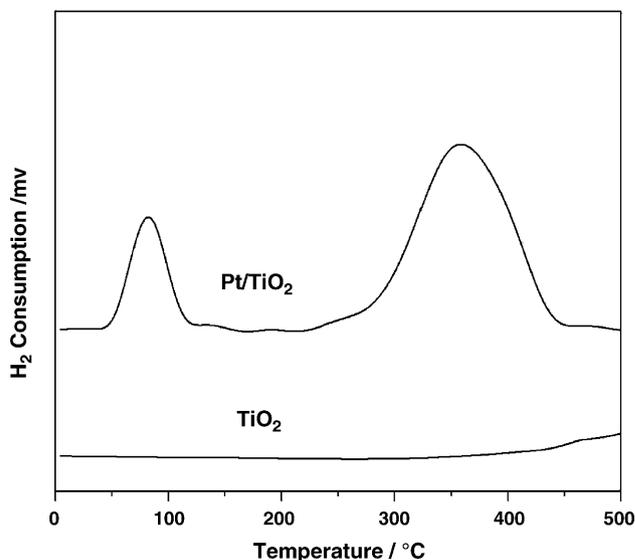
Fig. 6. Temperature programmed reduction (H$_2$-TPR) profiles of TiO$_2$ and 1% Pt/TiO$_2$ catalysts.

temperature. Further increase of Pt loading from 1 to 2% did not affect the HCHO conversion. Therefore, the optimal Pt loading was 1%.

3.1.3. Effect of GHSV

Fig. 3 shows the conversions of HCHO at room temperature as a function of reaction time over 1% Pt/TiO$_2$ at GHSVs of 50,000, 100,000 and 200,000 h^{-1}. The steady conversions of HCHO were 100% at 50,000 h^{-1}, 97% at 100,000 h^{-1} and 58% at 200,000 h^{-1}. In addition, after the HCHO conversion reached the steady level, there was no indication of deactivation during the period of investigation (24 h).

After the HCHO conversion reached a steady level at GHSVs of 50,000, 100,000 and 200,000 h^{-1}, the mass balance for the catalytic oxidation of HCHO over 1% Pt/TiO$_2$ at room temperature was recorded and is shown in Table 1.

Average values for the 10 runs at different GHSVs were used in Table 1. The concentration of 102 ppm HCHO became 0 and 102 ppm CO$_2$ was produced at GHSV of 50,000 h^{-1}. Similarly, the HCHO concentrations decreased from 101 (or 102 ppm) to 3 and 43 ppm at GHSVs of 100,000 and 200,000 h^{-1}, and 98.7 and 58.9 ppm CO$_2$ was produced, respectively. Therefore, we concluded that the catalytic oxidation of (HCHO + O$_2$) → (CO$_2$ + H$_2$O) strictly proceeded on the 1% Pt/TiO$_2$. It is worthy of note that no by-products were detected except a constant concentration of a small amount of CO in the effluent gas.
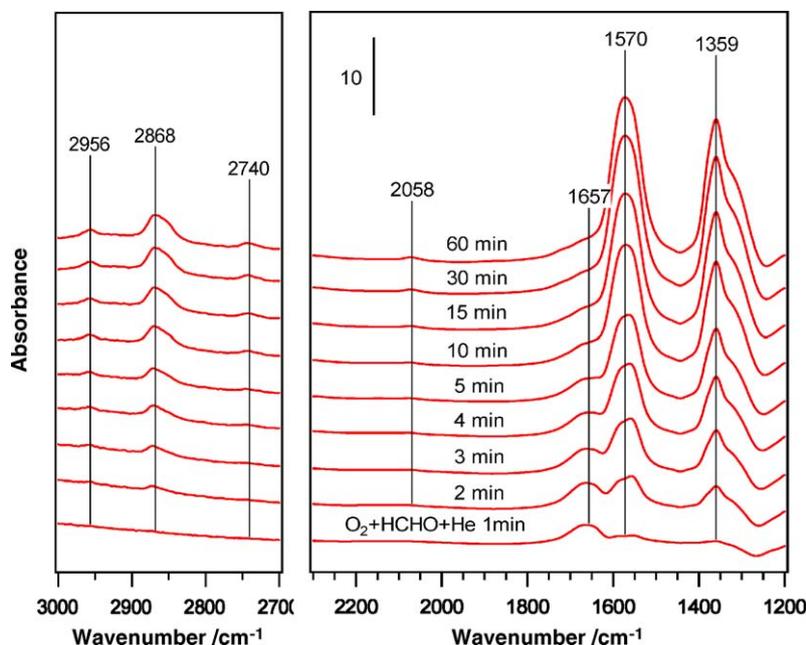
Fig. 7. Dynamic changes of in situ DRIFTS of the 1% Pt/TiO$_2$ catalyst as a function of time in a flow of O$_2$ + HCHO + He at room temperature.
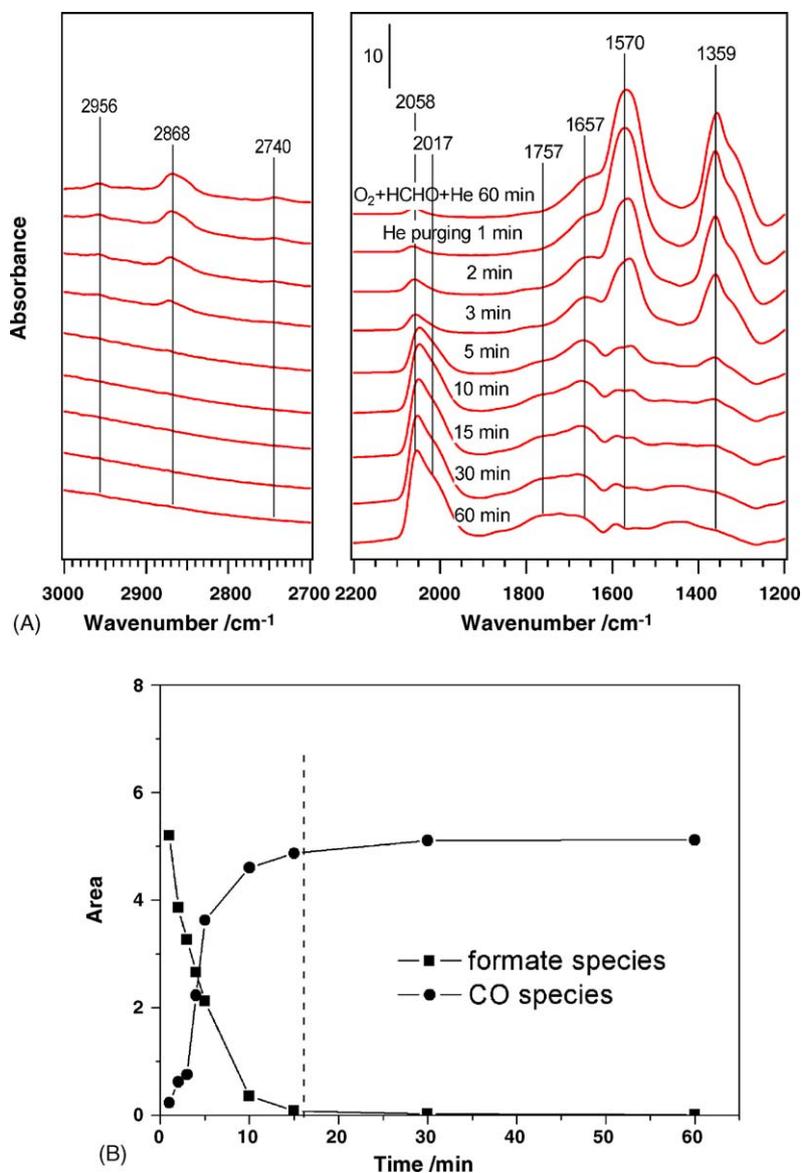
Fig. 8. (A) Dynamic changes of in situ DRIFTS of the 1% Pt/TiO$_2$ catalyst as a function of time in a flow of helium at room temperature after exposed catalyst to a flow of O$_2$ + HCHO + He for 60 min (Fig. 7). (B) Time dependence of the integrated areas of the peak in the range of 1490–1635 cm^{-1} (■, formate species) and 1920–2100 cm^{-1} (●, CO species).

3.2. Characterization of catalysts

BET surface areas of TiO$_2$ and the 1% Pt/TiO$_2$ catalysts are shown in Table 2. Compared to the bare TiO$_2$, surface area of 1% Pt/TiO$_2$ was slightly decreased. Deposit of 1% small Pt particles on TiO$_2$ resulted in about 4% reduction of the BET area.

Catalyst structures were revealed by XRD. Fig. 4 shows that the XRD pattern of the 1% Pt/TiO$_2$ catalyst is essentially the same as that of the TiO$_2$ sample (anatase type). The absence of diffraction lines of Pt phase on the 1% Pt/TiO$_2$ catalyst indicates that platinum is well dispersed. The high dispersion degree can also be confirmed by the HR TEM image of the 1% Pt/TiO$_2$ (Fig. 5), which exhibits a clear lattice image of TiO$_2$, but undistinguishable crystalline Pt particles on TiO$_2$. As the detection limit of the HR TEM technique is around 1 nm, the Pt particles on TiO$_2$ are probably dispersed into a size smaller than 1 nm, which could be very important for the high activity of this catalyst at room temperature.

Fig. 6 shows hydrogen temperature programmed reduction (H$_2$-TPR) profiles carried out on TiO$_2$ and 1% Pt/TiO$_2$ catalysts. Between 25 and 500 °C, no reduction peak was observed on the TiO$_2$ sample. It must be reminded that the reduction of bulk oxygen of TiO$_2$ has been reported to occur at $T > 600$ °C [22–24]. The Pt/TiO$_2$ sample showed two H$_2$-consumption peaks with a maximum at 80 and 360 °C. The H$_2$-consumption peak at around 80 °C was associated to the reduction of PtO$_x$ crystallites to metallic Pt, and the peak at around 360 °C could be attributed to the reduction of the surface capping oxygen of TiO$_2$ [24–26]. These results suggest that the presence of Pt facilitates the reduction of oxygen

species on TiO_2 surface. Similar effect of noble metals (Au, Pt, Rh and Pd) was well known on CeO_2 [27,28].

3.3. In situ DRIFTS study

In order to investigate the mechanism of HCHO oxidation on 1% Pt/TiO_2, the transient DRIFTS experiments were performed.

Fig. 7 shows the changes in the DRIFTS spectra of Pt/TiO_2 catalyst as a function of time in a flow of O_2 + HCHO + He at room temperature. After the catalyst was exposed to O_2 + HCHO + He mixture gas at room temperature, the bands at 2956, 2868, 2740, 2058, 1657, 1570 and 1359 cm^{-1} appeared. With time increasing, the bands intensities increased and reached a steady level after 60 min. According to previous studies, two strong bands at 1570 and 1359 cm^{-1} were ascribed to $\nu_{as}(COO)$ and $\nu_s(COO)$ on TiO_2 sites [29–34]. The small bands at 2956, 2868 and 2740 cm^{-1} were assigned to $\nu(C–H)$ [30–34]. These spectra suggest that the adsorbed HCHO rapidly converts to formate species on the Pt/TiO_2 catalyst. A very weak band appearing at 2058 cm^{-1} is assignable to linear CO adsorbed on Pt [33,34], and the band at 1657 cm^{-1} is due to water adsorbed on the catalyst (originated from the moisture in reactant gases). However, there is no peak associated to molecularly adsorbed HCOOH and HCHO on the catalyst in the flow of HCHO + O_2 + He at room temperature [33–35]. It is noteworthy that the formate species did not appear on pure TiO_2 at the same conditions (data are not shown), indicating that the Pt addition promotes the formation of formate species.

After Pt/TiO_2 catalyst was exposed to a flow of O_2 + HCHO + He for 60 min, the sample was purged by He. The changes in the DRIFTS spectra of Pt/TiO_2 catalyst are shown in Fig. 8A. The integrated areas of the bands in Fig. 8A are displayed as a function of time in Fig. 8B. Noticeably, the bands of formate species (2956, 2868, 2740, 1570 and 1359 cm^{-1}) decreased, and almost disappeared after purged for about 15 min. Meanwhile, two strong bands (2058 and 2017 cm^{-1}) and a broad band (1757 cm^{-1}) appeared, and these bands could be assigned to linearly adsorbed CO (2058 and 2017 cm^{-1}) and bridge adsorbed CO (1757 cm^{-1}) on Pt metal particles [33–35]. Taking these results into account, we believe that the decomposition of surface formate species into linearly adsorbed CO and bridge adsorbed CO occurs at room temperature in the absence of O_2. The reactivity of adsorbed CO toward O_2 was also studied by in situ DRIFTS. The dynamic changes of in situ DRIFTS of the CO/Pt/TiO_2 as a function of time in a flow of O_2 are shown in Fig. 9. The adsorbed CO bands rapidly decreased and completely disappeared in 10 min, indicating that the adsorbed CO species was extremely reactive toward O_2 even at room temperature. It is necessary to point out that CO consuming rate must be faster than its forming rate under the reaction conditions, and thereby, little adsorbed CO species was observed on Pt/TiO_2 catalyst in the flow of O_2 + HCHO + He as shown in Fig. 7. In addition, the results suggest that the conversion of surface formate to adsorbed CO on the catalyst is probably the rate-determining step for the catalytic oxidation of HCHO on the 1% Pt/TiO_2 catalyst.

On the basis of these obtained results, Fig. 10 gives a simplified reaction scheme for the catalytic oxidation of HCHO on the 1% Pt/TiO_2 catalyst at room temperature. HCHO firstly is oxidized into formate surface species at room temperature. Formate surface species then directly decompose into adsorbed CO species and H_2O, and the CO species finally reacts with O_2 to produce CO_2.
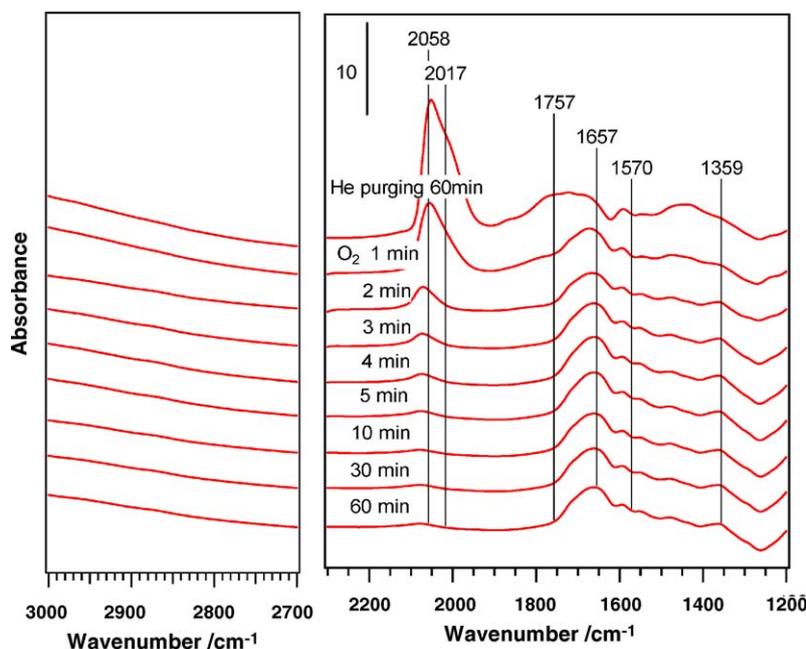
Fig. 9. Dynamic changes of in situ DRIFTS of the CO/Pt/TiO_2 as a function of time in a flow of O_2 at room temperature after the sample was purged by He for 60 min (shown in Fig. 8).

$$M: Pt/TiO_2$$

$$HCHO \xrightarrow{\text{O-M}} HCOO + H \longrightarrow CO + H_2O \xrightarrow{\text{O}_2} CO_2 + M$$
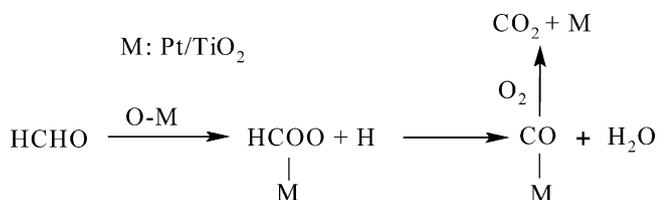
Fig. 10. Reaction scheme of the catalytic oxidation of HCHO on 1% Pt/TiO$_2$ catalyst at room temperature.

4. Conclusions

Pt/TiO$_2$ is found to be the most active catalyst among TiO$_2$ supported noble metal (Pt, Rh, Pd and Au) catalysts for HCHO oxidation. The optimal Pt loading of Pt/TiO$_2$ is 1%. HCHO can be completely oxidized into CO$_2$ and H$_2$O over 1% Pt/TiO$_2$ at GHSV of 50,000 h^{-1} at room temperature. XRD patterns and HR TEM image indicate that Pt is in a very high dispersion degree on TiO$_2$, which is presumably a very important reason for the high activity of Pt/TiO$_2$. Formate and adsorbed CO species are the reaction intermediates. The conversion of surface formate to adsorbed CO on the catalyst is the rate-determining step for the catalytic oxidation of HCHO over the Pt/TiO$_2$ catalyst.

Acknowledgements

References

[1] C. Yu, D. Crump, Build. Environ. 33 (1998) 357.
[2] J.J. Collins, R. Ness, R.W. Tyl, N. Krivanek, N.A. Esmen, T.A. Hall, Regul. Toxicol. Pharm. 34 (2001) 17.
[3] B. Eriksson, L. Johanssin, I. Svedung, The Nordest Symposium on Air Pollution Abatement by Filtration and Respiratory Protection, Copenhagen, 1980.
[4] Arthur D. Little Inc., A Report to the HCHO Institute by Arthur D. Little Inc., Cambridge, MA, 1981.
[5] Y. Sekine, A. Nishimura, Atmos. Environ. 35 (2001) 2001.
[6] J.J. Spivey, Ind. Eng. Chem. Res. 26 (1987) 2165.
[7] S. Scirè, S. Minicò, C. Crisafulli, C. Satriano, A. Pistone, Appl. Catal. B: Environ. 40 (2003) 43.
[8] S. Scirè, S. Minicò, C. Crisafulli, S. Galvagno, Catal. Commun. 2 (2001) 229.
[9] J.E. Sawyer, M.A. Abraham, Ind. Eng. Chem. Res. 33 (1994) 2084.
[10] P. Papaefthimiou, T. Ioannides, X.E. Verykios, Catal. Today 54 (1999) 81.
[11] W. Wang, H.B. Zhang, G.D. Lin, Z.T. Xiong, Appl. Catal. B: Environ. 24 (2000) 219.
[12] E.M. Cordi, J.L. Falconer, Appl. Catal. A: Gen. 15 (1997) 179.
[13] J.M. Saleh, S.M. Hussian, J. Chem. Soc., Faraday Trans. 82 (1986) 2221.
[14] S. Imamura, D. Uchihori, K. Utani, Catal. Lett. 24 (1994) 377.
[15] M.C. Álvarez-Galván, V.A. de la Peña O'Shen, J.L.G. Fierro, P.L. Arias, Catal. Commun. 4 (2003) 223.
[16] E.M. Cordi, P.J. O'Neill, J.L. Falconer, Appl. Catal. B: Environ. 14 (1997) 23.
[17] P.O. Larsson, A. Andersson, Appl. Catal. B: Environ. 24 (2000) 175.
[18] C. Mazzocchia, A. Kaddouri, J. Mol. Catal. A: Chem. 204–205 (2003) 647.
[19] S.C. Kim, J. Hazard. Mater. 91 (2002) 285.
[20] Y. Sekine, Atmos. Environ. 36 (2002) 5543.
[21] C.B. Zhang, H. He, K. Tanaka, Catal. Commun. 6 (2005) 211.
[22] X.Y. Jiang, G.H. Ding, L.P. Lou, Y.X. Chen, X.M. Zheng, J. Mol. Catal. A: Chem. 218 (2004) 187.
[23] J.A. Wang, A. Cuan, J. Salmones, N. Nava, S. Castillo, M. Morán-Pineda, F. Rojas, Appl. Surf. Sci. 230 (2004) 94.
[24] N.S. de Resende, J.-G. Eon, M. Schmal, J. Catal. 183 (1999) 6.
[25] W.S. Epling, P.K. Cheekatamarla, A.M. Lane, Chem. Eng. J. 93 (2003) 61.
[26] R. Pérez-Hernández, A. Gómez-Cortés, J. Arenas-Alatorre, S. Rojas, R. Mariscal, J.L.G. Fierro, G. Díaz, Catal. Today 107–108 (2005) 149.
[27] A. Trovarelli, G. Dolcetti, C. De Leitenburg, J. Kaspar, P. Finetti, A. Santoni, J. Chem. Soc., Faraday Trans. 88 (1992) 1311.
[28] H.C. Yao, Y.F. Yao, J. Catal. 86 (1984) 254.
[29] F. Boccuzzi, A. Chiorino, M. Manzoli, J. Power Sources 118 (2003) 304.
[30] G.J. Millar, C.H. Rochester, K.C. Waugh, J. Catal. 155 (1995) 52.
[31] F.Z. Liu, M.M. Yang, W. Zhou, Z.Y. Jiang, Electrochem. Commun. 5 (2003) 276.
[32] G.Y. Popova, Y.A. Chesalov, T.V. Andrushkevich, I.I. Zakharov, E.S. Stoyanov, J. Mol. Catal. A: Chem. 158 (2000) 345.
[33] J. Raskó, T. Kecskés, J. Kiss, J. Catal. 224 (2004) 261.
[34] T. Kecskés, J. Raskó, J. Kiss, Appl. Catal. A: Gen. 273 (2004) 55.
[35] J. Raskó, J. Catal. 217 (2003) 478.